BULLETIN OF THE EARTHQUAKE
RESEARCH INSTITUTE
Vol. 40 (1962), pp. 657-683

36. *Electromagnetic Induction within an Anisotropic Plane Sheet over a Non-conductor and Underlain by a Uniform Semi-infinite Conductor.*

By Tsuneji RIKITAKE,

Earthquake Research Institute

and

Munehisa SAWADA,

Graduate School, University of Tokyo.

(Read July 24, 1962.—Received Sept. 29, 1962.)

Summary

Electromagnetic induction within an anisotropic plane sheet over a non-conductor and underlain by a uniform semi-infinite conductor is studied in the hope of describing time-dependent earth-currents properly. It is made clear that the direction of the maximum electric field in the sheet does not generally agree with those of the induced electric current or the maximum resistivity. The induced fields, both electric and magnetic, are influenced very little by the deep-seated conductor in the case of rapid variation. The effect of the high conductivity in the deep-seated conductor becomes appreciable for slow variations provided their wave-lengths are much larger than the depth of the conducting layer. The rapid-run data observed at Kakioka Magnetic Observatory during the International Geophysical Year are analysed on the basis of the theory developed here.

1. Introduction

In spite of the long history of observation, there are still a number of elusive problems relating to earth-currents as has been recently summarized by T. Yoshimatsu[1]. Although it has been established that most of time-dependent parts of earth-currents are caused by electromagnetic induction within the earth by a time-dependent magnetic field originating from outside the earth, the reason why changes in earth-currents generally predominate in a certain direction is not quite clear.

1) T. YOSHIMATSU, *Mem. Kakioka Mag. Obs. Suppl.*, **1** (1957).

This kind of apparent anisotropy has been presumed to be caused by non-uniform distribution of resistivity around the observation point though no general relationship between maximum direction of earth-currents and topography or geological structure has been established.

A number of theories of earth-currents based on electromagnetic induction within the earth have been put forward in relation to "magneto-tellurics"[1),2),3),4)] though they are by no means satisfactory as critically reviewed by A. T. Price[5)]. It seems to the authors that an electromagnetic induction theory within an anisotropic earth with proper considerations for boundary conditions has never been developed. It is the intention of this paper to advance a theory of electromagnetic induction within an anisotropic earth in a form suitable for discussing earth-currents.

We assume a plane earth, the surface of which is covered by a thin sheet of anisotropic conductivity. The assumption may be justified so long as the near-surface irregularities in the electrical coductivity play an important role on earth-currents. It is further assumed that the sheet lies on a non-conducting layer of a few hundred kilometers in thickness which is also underlain by a semi-infinite medium of unifom conducivity. According to S. Chapman[6),7)], A. T. Price[7),8)], B. N. Lahiri[8)] and T. Rikitake[9)] who applied electromagnetic induction theory to the analyses of transient geomagnetic changes, the conductivity takes a very low value of the order of 10^{-15} *e. m. u.* down to a depth of some 400 *km* while it amounts to 10^{-12} *e. m. u.* or more in the part of the earth below this level. Since it is of importance and interest to see to what extent the earth-currents at the earth's surface are affected by the deeper layer, the distribution of electrical conductivity thus surmised is also taken into account in the present theory.

In order to demonstrate how well the theory can be applied to an analysis of earth-current data, the quick-run tellurigrams as well as magnetograms, published by Kakioka Magnetic Observatory[10)], during the International Geophysical Year are analyzed, the apparent anisotropy

2) L. CAGNIARD, *Geophysics*, **18** (1953), 605.
3) Y. KATO and T. KIKUCHI, *Sci. Rep. Tohoku Univ.*, Ser. V, **2** (1950), 139.
4) T. RIKITAKE, *Bull. Earthq. Res. Inst.*, **29** (1951), 271.
5) A. T. PRICE, *Journ. Geophys. Res.*, **67** (1962), 1907.
6) S. CHAPMAN, *Phil. Trans. Roy. Soc. London A*, **218** (1919), 1.
7) S. CHAPMAN and A. T. PRICE, *Phil. Trans. Roy. Soc. London A*, **229** (1930), 427.
8) B. N. LAHIRI and A. T. PRICE, *Phil. Trans. Roy. Soc. London A*, **237** (1939), 509.
9) T. RIKITAKE, *Bull. Earthq. Res. Inst.*, **28** (1950), 45, 219 and 263.
10) KAKIOKA MAGNETIC OBSERVATORY, *Rep. Geomagn. Geoelectr. Obs. IGY*, (1960).

of the resistivity at Kakioka being approximately determined on the basis of the present theory.

2. Model of the earth and inducing field

Let us assume that only the outermost layer of the earth is anisotropic, so that the layer may be regarded as an infinitesimally thin sheet. Beneath the anisotropic sheet, we assume a non-conducting layer of thickness H which is also underlain by a uniform isotropic semi-infinite conductor. The model of the earth is then illustrated as shown in Fig. 1.

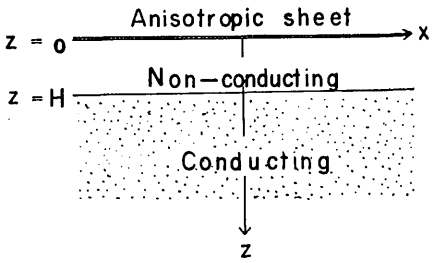

Fig. 1. Model of the earth.

The magnetic potential of the inducing field that originates from outside the earth is assumed to be expressed as

$$W_e = ee^{-rz}\cos r\eta\ , \qquad (1)$$

where (ξ, η) denotes a rectangular coordinate-system in the xy-plane as shown in Fig. 2. Since we have relations

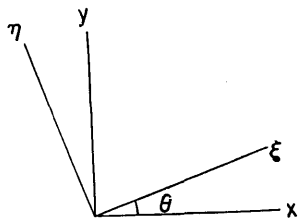

Fig. 2. The relation between the two coordinate-systems. The maximum and minimum directions of resistivity are taken as the x and y axes respectively, while the direction of the inducing field is taken parallel to the η axis in the later work.

$$\left.\begin{aligned}\xi &= x\cos\theta + y\sin\theta\\ \eta &= -x\sin\theta + y\cos\theta\end{aligned}\right\}, \qquad (2)$$

(1) can be written as

$$W_e = ee^{-rz}(\cos px\cos qy + \sin px\sin qy)\ , \qquad (3)$$

where

$$p = r\sin\theta\ , \qquad q = r\cos\theta\ . \qquad (4)$$

3. Theoy of electromagnetic induction

In the non-conducting regions, we may define magnetic potential W which satisfies

$$\nabla^2 W = 0\ . \qquad (5)$$

Taking into consideration the fact that the inducing field is given by (3), the solution of (5) for harmonic constituent $\cos px \cos qy$ is obtained as

$$W=(ee^{-rz}+ie^{rz})\cos px\cos qy \qquad \text{for } z<0 \tag{6}$$

and

$$W=(e'e^{-rz}+i'e^{rz})\cos px\cos qy \qquad \text{for } 0<z<H\,. \tag{7}$$

As long as the anisotropy is constant throughout the sheet, it is obvious that the induced field is expressible with the harmonic constituent which is the same as that for the inducing field. Attention should be drawn, however, to the induction in a non-uniform sheet. In that case, many other constituents necessarily come out.

The solution of (5) for $\sin px \sin qy$ is also obtained in a form similar to (6) and (7), so that only the theory for the inducing potential proportional to $\cos px \cos qy$ is developed below. The three components of magnetic field become

$$\left.\begin{aligned} H_x&=p(ee^{-rz}+ie^{rz})\sin px\cos qy\\ H_y&=q(ee^{-rz}+ie^{rz})\cos px\sin qy\\ H_z&=r(ee^{-rz}-ie^{rz})\cos px\cos qy \end{aligned}\right\} \qquad \text{for } z<0 \tag{8}$$

and

$$\left.\begin{aligned} H_x&=p(e'e^{-rz}+i'e^{rz})\sin px\cos qy\\ H_y&=q(e'e^{-rz}+i'e^{rz})\cos px\sin qy\\ H_z&=r(e'e^{-rz}-i'e^{rz})\cos px\cos qy \end{aligned}\right\} \qquad \text{for } 0<z<H\,. \tag{9}$$

In the conducting region for $H<z$ (conductivity: σ), we take vector potential $\vec{A}$ which satisfies

$$\nabla^2\vec{A}=4\pi\sigma\partial\vec{A}/\partial t\,. \tag{10}$$

The magnetic permeability is assumed as unity in electromagnetic units everywhere. The three components of the appropriate solution of (10) are given as

$$\vec{A}=\begin{cases} qCe^{-\sqrt{r^2+\kappa^2}z}\cos px\sin qy\\ -pCe^{-\sqrt{r^2+\kappa^2}z}\sin px\cos qy\\ 0 \end{cases} \tag{11}$$

in which, putting $\partial/\partial t=D$, we write

$$\kappa^2=4\pi\sigma D\,. \tag{12}$$

Applying relation curl $\vec{A}=\vec{H}$ to (11), the three components of magnetic field are obtained as

$$\left.\begin{aligned} H_x &= prCe^{-\sqrt{r^2+\kappa^2}z}\sin px\cos qy \\ H_y &= qrCe^{-\sqrt{r^2+\kappa^2}z}\cos px\sin qy \\ H_z &= r^2Ce^{-\sqrt{r^2+\kappa^2}z}\cos px\cos qy \end{aligned}\right\} \quad \text{for } H<z\,. \tag{13}$$

When there is a current sheet at $z=0$ and its current function is assumed to be expressed as

$$\Psi = K_c\cos px\cos qy\,, \tag{14}$$

the continuity condition of magnetic field at $z=0$ leads to

$$\left.\begin{aligned} e+i &= e'+i'+4\pi K_c \\ e-i &= e'-i' \end{aligned}\right\}, \tag{15}$$

while the similar condition at $z=H$ leads to

$$\left.\begin{aligned} e'e^{-rH}+i'e^{rH} &= C\sqrt{r^2+\kappa^2}e^{-\sqrt{r^2+\kappa^2}H} \\ e'e^{-rH}+i'e^{rH} &= Cre^{-\sqrt{r^2+\kappa^2}H} \end{aligned}\right\}. \tag{16}$$

Solving (16) with regard to e' and i', we obtain

$$\left.\begin{aligned} e' &= \frac{1}{2}C(\sqrt{r^2+\kappa^2}+r)e^{-(\sqrt{r^2+\kappa^2}-r)H} \\ i' &= \frac{1}{2}C(\sqrt{r^2+\kappa^2}-r)e^{-(\sqrt{r^2+\kappa^2}+r)H} \end{aligned}\right\}. \tag{17}$$

Putting (17) into (15) and solving it with respect to e and i, we get

$$\left.\begin{aligned} e &= 2\pi K_c+\frac{1}{2}C(\sqrt{r^2+\kappa^2}+r)e^{-(\sqrt{r^2+\kappa^2}-r)H} \\ i &= 2\pi K_c+\frac{1}{2}C(\sqrt{r^2+\kappa^2}-r)e^{-(\sqrt{r^2+\kappa^2}+r)H} \end{aligned}\right\}. \tag{18}$$

Since e is given as the coefficient of the inducing field, the first equation of (18) specifies the relation between K_c and C. If K_c is obtained by some means, it is possible to obtain i in terms of e from the second equation of (18).

We are now in a position to determine K_c in the following. According to the theory of electromagnetic induction in a sheet, the

condition that should be satisfied in an anisotropic sheet is obtained as follows.

The relation between electric field $\vec{E}_s$ and electric current density $\vec{i}_s$ in the sheet, both parallel to the sheet, is given as

$$\vec{E}_s=(\rho)\vec{i}_s ,$$

where (ρ) is the resistivity which is generally given by a tensor like

$$(\rho)=\begin{pmatrix}\rho_{xx} & \rho_{xy}\\ \rho_{yx} & \rho_{yy}\end{pmatrix} .$$

In that case, the z component of curl $\vec{E}_s$ is calculated as

$$(\text{curl}\,\vec{E}_s)_z=\rho_{yx}\frac{\partial i_{sx}}{\partial x}+\rho_{yy}\frac{\partial i_{sy}}{\partial x}-\rho_{xx}\frac{\partial i_{sx}}{\partial y}-\rho_{xy}\frac{\partial i_{sy}}{\partial y} .$$

As $\text{div}\,\vec{i}_s=0$, we may make use of a current function Ψ by which the components of $\vec{i}_s$ are give as

$$i_{sx}=-\frac{\partial\Psi}{\partial y} , \quad i_{sy}=\frac{\partial\Psi}{\partial x} .$$

It then follows that

$$\rho_{yy}\frac{\partial^2\Psi}{\partial x^2}-(\rho_{xy}+\rho_{yx})\frac{\partial^2\Psi}{\partial x\partial y}+\rho_{xx}\frac{\partial^2\Psi}{\partial y^2}=-\frac{\partial H_z}{\partial t} \qquad (19\,a)$$

from Maxwell's relation $(\text{curl}\,\vec{E}_s)_z=-\frac{\partial H_z}{\partial t}$. This is the condition that should be satisfied at $z=0$.

Assuming that the resistivity tensor is symmetric and that the principal axes are directed to the x and y axes, (19 a) reduces to

$$\rho_{yy}\frac{\partial^2\Psi}{\partial x^2}+\rho_{xx}\frac{\partial^2\Psi}{\partial y^2}=-\frac{\partial H_z}{\partial t} . \qquad (19\,b)$$

Putting (14) and the last expression of (8) into (19 b), we obtain

$$(\rho_{yy}p^2+\rho_{xx}q^2)K_c=Dr(e-i) , \qquad (20)$$

in which $e-i$ can be, with the aid of (18), replaced by

$$e-i=\frac{1}{2}C\{(\sqrt{r^2+\kappa^2}+r)e^{rH}-(\sqrt{r^2+\kappa^2}-r)e^{-rH}\}e^{-\sqrt{r^2+\kappa^2}H} ,$$

which is also written as

$$e-i=\left\{1-\frac{\sqrt{r^2+\kappa^2}-r}{\sqrt{r^2+\kappa^2}+r}e^{-2rH}\right\}(e-2\pi K_c)\ . \tag{21}$$

Substituting (21) into (20), we obtain

$$(\rho_{yy}p^2+\rho_{xx}q^2)K_c=Dr(e-2\pi K_c)\left\{1-\frac{\sqrt{r^2+\kappa^2}-r}{\sqrt{r^2+\kappa^2}+r}e^{-2rH}\right\}\ . \tag{22}$$

This is the equation solving which we may have K_c in terms of e. A condition exactly the same as (22) can also be obtained for coefficient K_s of the current function for $\sin px \sin qx$. We write hereafter $K_c=K_s=K$, so that, solving (22), we obtain

$$K=\frac{DrMe}{\rho_{yy}p^2+\rho_{xx}q^2+2\pi rDM}\ , \tag{23}$$

where

$$M=1-\frac{\sqrt{r^2+\kappa^2}-r}{\sqrt{r^2+\kappa^2}+r}e^{-2rH}\ . \tag{24}$$

With the aid of K thus obtained, we can estimate all the electric and magnetic elements in the system.

4. Induction in an anisotropic plane sheet placed in free space

Let us first assume $\sigma=0$, so that the conducting semi-infinite medium is non-existing in this case. Thus we see that $M=1$ from (24) and that K is simplified as

$$K=\frac{Dre}{\rho_{yy}p^2+\rho_{xx}q^2+2\pi rD}\ . \tag{25}$$

In the case of a purely periodic change, we put

$$D=i\alpha\ , \qquad \alpha=2\pi/T \tag{26}$$

where T is the period. (25) can be then rewritten as

$$K/e=\frac{i\alpha}{r(\rho_{yy}\sin^2\theta+\rho_{xx}\cos^2\theta)+2\pi i\alpha}\ . \tag{27}$$

Assuming, for example, that the sheet is composed of a substance

with specific conductivity 10^{-12} *e. m. u.* in the direction parallel to the y axis and also that the thickness of the sheet amounts to 10 *km*, we take

$$\rho_{yy}=10^{6}\ e.\ m.\ u.\ .$$

It is further assumed that the resistivity contrast between y and x directions amounts to 10, so that

$$\rho_{xx}=10^{5}\ e.\ m.\ u.\ .$$

With these resistivity values, K/e as given in (27) is calculated for various θ's taking T as parameter, while the wave-length of the field is taken as 1000 *km*. Modulus and argument of K/e, that is the amplitude ratio and phase difference between K and e, are then calculated as shown in polar diagrams Figs. 3 and 4.

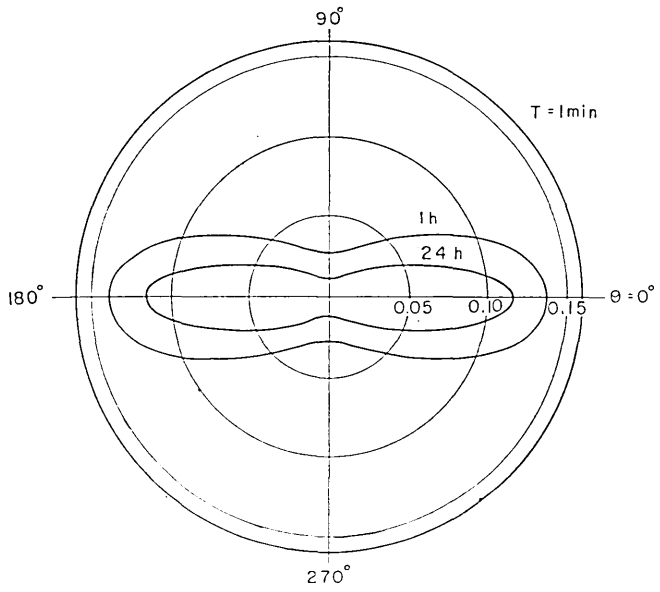

Fig. 3. Amplitude ratio K/e for $T=1\,min.$, $1\,h$ and $24\,h$ in the case of the sheet placed in free space. The curve for $T=1\,min.$ is nearly circular, while the amplitude for $T=24\,h$ is enlarged ten times.

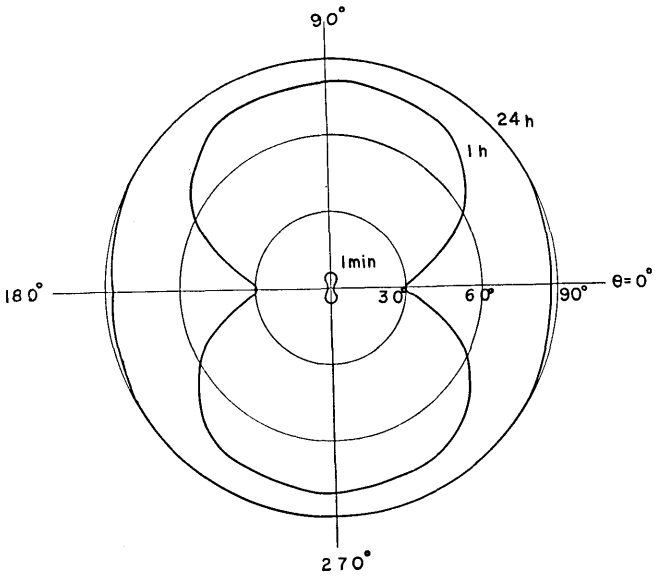

Fig. 4. Phase difference between K and e for $T=1\,min.$, $1\,h$ and $24\,h$ in the case of the sheet placed in free space.

Corresponding to the inducing field as given in (1), the current function becomes

$$\Psi = K\cos r\eta\ , \tag{28}$$

so that we see that the induced currents flow in a direction perpendicular to the inducing magnetic field. The intensity of induced currents changes according as the direction of the inducing field changes, the maximum occurring when the field changes in the direction of the lowest resistivity. It should be noticed that, when the inducing field changes very rapidly, very small anisotropy can be seen in the current intensity because the effect of self-induction becomes large in this case. When the period of the inducing field gets larger, the behaviour of induced currents approaches that of steady flow of current driven by a constant electromotive force whereas the effect of anisotropy in the resistivity is becoming greater.

The x and y components of the induced current intensity are obtained by differentiating Ψ with respect to y and x as

$$\left.\begin{aligned} i_x &= Kp\sin r\eta\ , \\ i_y &= Kq\sin r\eta\ . \end{aligned}\right\} \tag{29}$$

The components of the electric field in the directions of the principal axes then become

$$\left.\begin{aligned} E_x &= \rho_{xx} i_x = \rho_{xx} Kq \sin r\eta \\ E_y &= \rho_{yy} i_y = \rho_{yy} Kp \sin r\eta \end{aligned}\right\}, \tag{30}$$

so that the ξ and η components are obtained by relation

$$\left.\begin{aligned} E_\xi &= E_x \cos\theta + E_y \sin\theta \\ E_\eta &= -E_x \sin\theta + E_y \cos\theta \end{aligned}\right\}, \tag{31}$$

resulting in

$$\left.\begin{aligned} E_\xi &= rK(\rho_{xx}\cos^2\theta + \rho_{yy}\sin^2\theta)\sin r\eta\ , \\ E_\eta &= -rK(\rho_{xx}-\rho_{yy})\sin\theta\cos\theta\sin r\eta\ . \end{aligned}\right\} \tag{32}$$

We therefore see that an electric field parallel to the inducing magnetic field comes into existence except for $\theta=0°$ and $90°$ In Figs. 5 and 6 are shown the directional characteristics of amplitudes of E_ξ

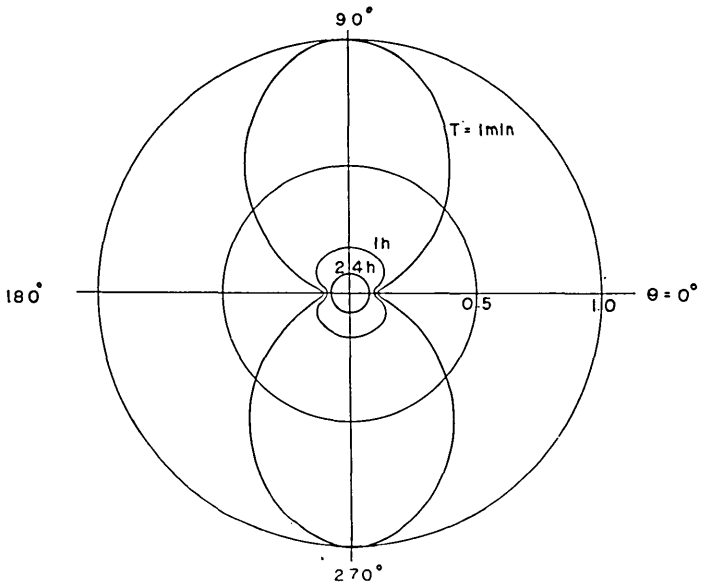

Fig. 5. Directional characteristics of E_ξ (the electric field perpendicular to the inducing magnetic field) in an arbitrary scale for the sheet placed in free space. The amplitude for $T=24h$ is enlarged ten times.

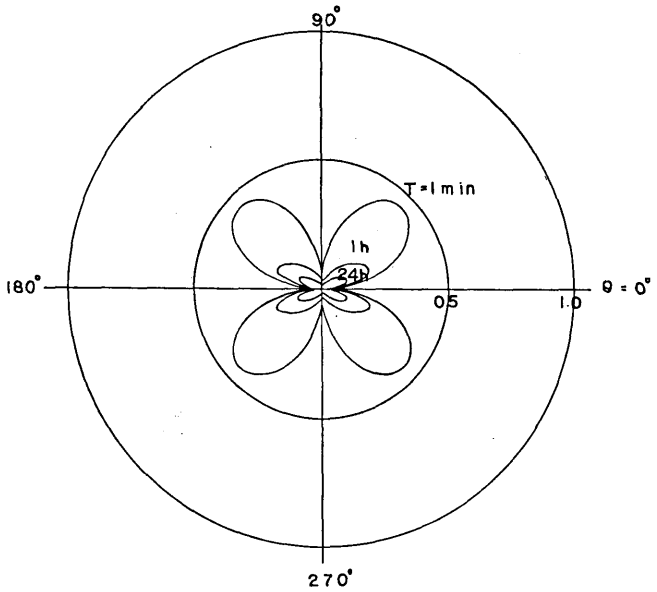

Fig. 6. Directional characteristics of E_η (the electric field parallel to the inducing magnetic field) in an arbitrary scale for the sheet placed in free space. The amplitude for $T=24h$ is enlarged ten times.

and E_η in the same arbitrary scale. The maximum of E_ξ, the electric field perpendicular to the direction of the magnetic field, takes place when the electric field is directed in the direction of the highest resistivity. For a rapid change, E_ξ exhibits a large anisotropy as can be seen in Fig. 5. Meanwhile the anisotropy becomes very small for a relatively slow change of 1-day period or so.

It is important that the direction of the induced electric field differs from that of the induced current. The angle δ between the two vectors as defined by

$$\delta=\tan^{-1}(E_\eta/E_\xi)\ , \tag{33}$$

which is independent of the period of the inducing field, changes as shown in Fig. 7 according as the direction of the inducing field changes. The maximum deviation, that occurs when θ is around 20°, is about 55° in the present case.

It is also of interest to examine in which direction the maximum and minimum of the electric field appear. For that purpose a polar diagram for $(E_\xi^2+E_\eta^2)^{1/2}$ is drawn as can be seen in Fig. 8 using a

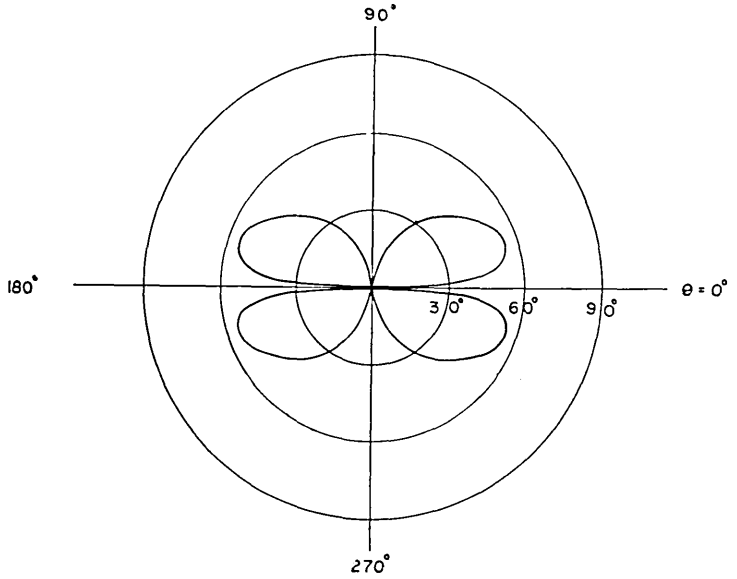

Fig. 7. Directional characteristics of δ for the sheet placed in free space. The angle between the induced electric field and current is given by $\delta-\theta$.

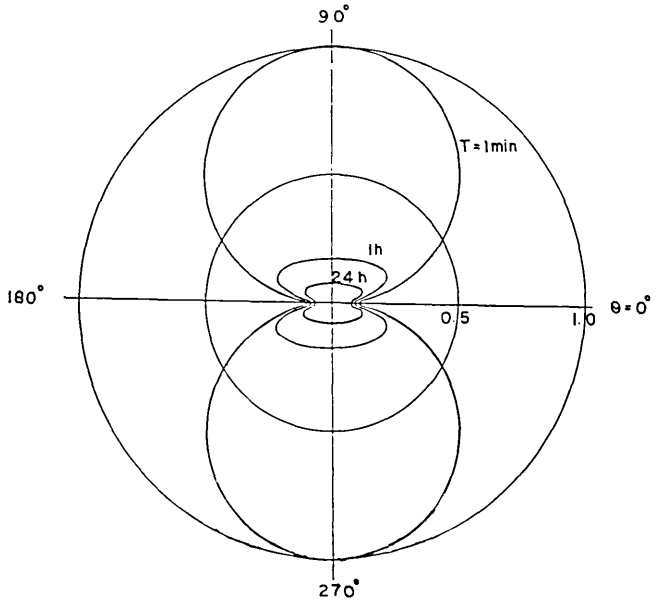

Fig. 8. Directional characteristics of $(E_\xi^2+E_\eta^2)^{1/2}$ (total amplitude of the electric field) in a scale which is the same as that in Figs. 5 and 6 for the sheet placed in free space. The amplitude for $T=24\,h$ is enlarged ten times.

scale the same as that of Figs. 5 and 6. We see that the minimum is always occurring in the $\theta=0°$ direction which is perpendicular to the direction of the inducing magnetic field, while the direction for the maximum electric field is not always constant. As can be seen in Fig. 8, the maxima for $T=1\,min.$, $1\,h$ and $24\,h$ take place when $\theta=90°$, $27°$ and $17°$ respectively. The point that the electric field does not necessarily become maximum when the inducing magnetic field is perpendicular to the direction of the highest resistivity is important.

From what we have been dealing with in this section, it is seen that, as far as induction in an anisotropic sheet is concerned, the direction of the induced electric field generally differs either from that of the induced currents which always flow perpendicularly to the inducing magnetic field or from that of the highest resistivity. It seems to the authors that there have been considerable misunderstandings in interpretation of earth-current observation. It has been customary to determine the direction in which electric field variations predominate. Some think that the induced currents are flowing in this direction. This is completely wrong in the case of an anisotropic earth. Others believe that the direction shows the direction of the highest resistivity. This also is not true. As long as the anisotropy in earth-current observation is assumed to be caused by electromagnetic induction in an anisotropic sheet, the situation is a little more complicated.

It has been sometimes reported that the direction in which electric field variations predominate is different for variations of different period. As far as the present theory goes, the direction should be constant provided a value is specified for θ. There is a possibility, however, that θ or the direction of inducing magnetic field is different for different variations. If it is so, even the apparent disagreement between directions of electric field variations of different kinds may be understandable on the basis of the present model.

In mageto-tellurics, it is customary to compare $\vec{E}$ with $\vec{H}$. The ξ and η components of $\vec{E}$ have been given in (32). The components for $\vec{H}$ are easily obtained as

$$\left.\begin{aligned} H_\xi &= 0\ , \\ H_\eta &= r(e+2\pi K)\sin r\eta\ . \end{aligned}\right\} \tag{34}$$

We then have

$$\frac{E_\xi}{H_\eta}=\frac{i\alpha(\rho_{xx}\cos^2\theta+\rho_{yy}\sin^2\theta)}{r(\rho_{xx}\cos^2\theta+\rho_{yy}\sin^2\theta)+4\pi i\alpha}\ , \tag{35}$$

$$\frac{E_\eta}{H_\eta}=\frac{i\alpha(\rho_{yy}-\rho_{xx})\sin\theta\cos\theta}{r(\rho_{xx}\cos^2\theta+\rho_{yy}\sin^2\theta)+4\pi i\alpha}\,. \tag{36}$$

With the aid of these expressions, moduli of E_ξ/H_η and E_η/H_η are calculated for various periods taking θ as parameter. The results are shown in Figs. 9 and 10. It is again seen that the influence of anisotropy becomes markedly large for short-period variations.

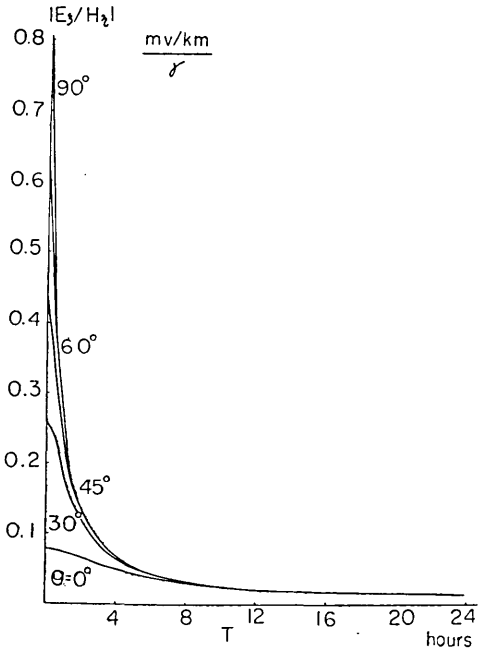

Fig. 9. $|E_\xi/H_\eta|-T$ relation for the sheet placed in free space.

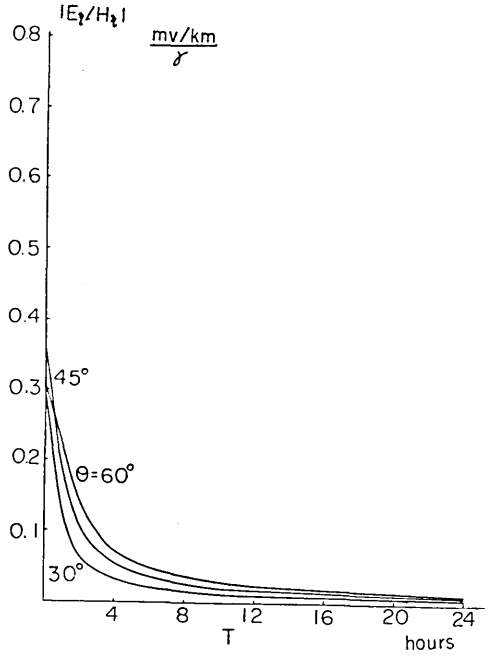

Fig. 10. $|E_\eta/H_\xi|-T$ relation for the sheet placed in free space.

5. Induction in an anisotropic plane sheet underlain by a uniform semi-infinite conductor

Let us take $\sigma=10^{-12}\,e.m.u.$ for the deep conductor and $H=400\,km$ as has been suggested by the previous studies[9]. Assuming the wavelength of the field to be $1000\,km$ as before, K is calculated while the resistivity values in the last section are also adopted.

The difference in K between the present case and the case for a sheet placed in free space as has been studied in the last section is

very small, so that the influence of the underlying conductor can be ignored in this case. The fact that the current intensity in both the cases becomes almost the same suggests that the coefficient of magnetic potential i is negligibly small at $z=0$. Although the magnetic potential arising from within the underlying conductor amounts to some fraction of the inducing one at $z=H$, it is seen that the magnetic field of this origin becomes very small at $z=0$. Going back to (24), factor e^{-2rH} takes a value as small as 0.007 for the wave-length and depth of the conductor adopted here, so that M differs very little from 1 for any combination of σ and T.

For actual geomagnetic variaions such as *ssc*, *si* and *sfe*, the wave-length supposed above seems to be too small though no exact estimate of wave-length is possible because of the earth's curvature. The authors would here like to demonstrate the influence of the deep-seated conductor on the assumption that the wave-length amounts to 10000 *km* which is ten times larger than that assumed before. In Figs. 11 and 12 are shown mod. (K/e) for $T=1\,h$ and $24\,h$ for both the sheet placed in free space and that underlain by a conductor. For the latter case,

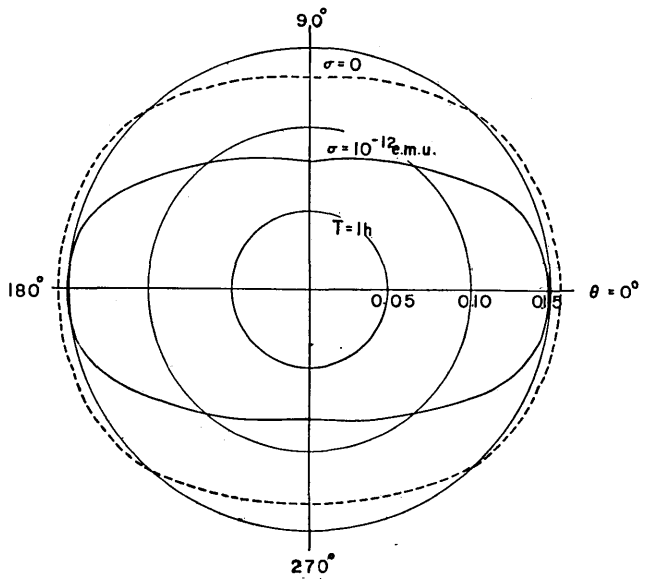

Fig. 11. Amplitude ratio (K/e) for $T=1\,h$. The curve denoted by $\sigma=0$ (broken line) is the one for the sheet placed in free space, while the curve denoted by $\sigma=10^{-12}\,e.m.u.$ (full line) is that for the sheet underlain by the conductor.

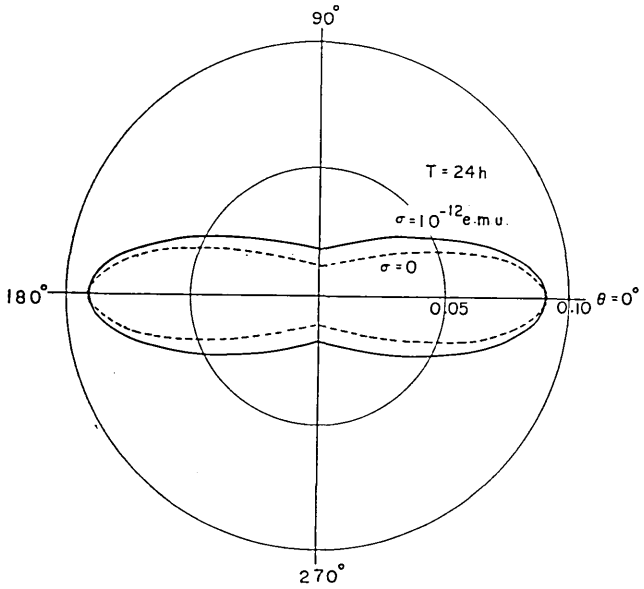

Fig. 12. Amplitude ratio (K/e) for $T=24\,h$. The curve denoted by $\sigma=0$ (broken line) is the one for the sheet placed in free space, while the curve denoted by $\sigma=10^{-12}\,e.m.u.$ (full line) is that for the sheet underlain by the conductor.

$\sigma=10^{-12}\,e.m.u.$ and $H=400\,km$ are assumed as before. The resistivity in the sheet is the same as that in the last section. mod. (K/e) for $T=1\,min.$ is almost the same as that shown in Fig. 3, so that we see that, when the sheet is placed either in free space or underlain by a conductor, the current intensity induced in the sheet is controlled very little by the wave-length in the case of a rapid variation. The influence of the deep layer is also very small in this case.

For slower variations, the influence of the underlying layer can be found in Figs. 11 and 12. It is interesting to note that the current induced in the sheet placed in free space is larger than that for the sheet underlain by the conducting layer in the case of a variation of medium period, $T=1\,h$ say, while the relation between the induced currents is reversed for a much slower variation like the one specified by $T=24\,h$. This may be understood when we take into consideration the fact that much current is induced in the deeper conductor in the case of a variation having a long period.

6. Analysis of rapid-run tellurigrams and magnetograms obtained at Kakioka Magnetic Observatory

During the International Geophysical Year, rapid-run observation of earth-currents as well as of geomagnetic fields were carried out at Kakioka Magnetic Observatory (latitude: 36.2° N, longitude: 140.2° E), Japan. The copies of tellurigrams and magnetograms published by the Observatory[10] provide a well-arranged set of data for testing the theory in this paper.

Among the data for 1958, fifteen examples listed in Table 1 are chosen for the analysis. They are *ssc*'s, *si*'s and *sfe*'s. These tellurigrams and magnetograms are read off every half a minute. These readings are made use of in drawing hodograms for both the magnetic ($\vec{H}$) and electric ($\vec{E}$) fields in the horizontal plane. Looking at the hodograms from Fig. 13 to Fig. 27 we see that the electric field always predominates in a direction slightly north of east. Yoshimatsu[1] has already mentioned that the direction in which the electric field at Kakioka exhibits its maximum is $N73°E$ for short period variation and $N60°E$ for S_q.

Table 1. List of the changes analysed.

No.	Time of occurrence				Remark
1	12*h*	12.5m *GMT*	Mar.	14	*ssc*
2	7	13	June	28	*ssc**
3	1	40	Aug.	24	*ssc*
4	10	5	Sept.	30	*ssc*
5	3	15	Oct.	22	*ssc**
6	7	29.5	Oct.	24	*ssc*
7	15	30	Mar.	3	*si*
8	13	44	Mar.	30	*si*
9	22	8.5	July	13	*si*
10	6	9	Aug.	27	*si*
11	4	9	Oct.	1	*si*
12	12	25	Dec.	13	*si*
13	4	53	Dec.	14	*si*
14	3	0	July	29	*sfe*
15	4	34	Aug.	16	*sfe*

It is not possible to infer how the inducing fields change only from the data at one observatory. We may assume, however, that as far as beginnings of disturbance are concerned coefficient e of inducing field changes as

$$e=\begin{cases} e_0(1-e^{-\lambda t}) & \text{for } t\geqq 0 \\ 0 & \text{for } t<0 \end{cases}. \tag{37}$$

In that case, it is obvious that K becomes

$$K=\frac{e_0}{2\pi}\frac{\lambda}{\lambda-\mu}(e^{-\mu t}-e^{-\lambda t}) \tag{38}$$

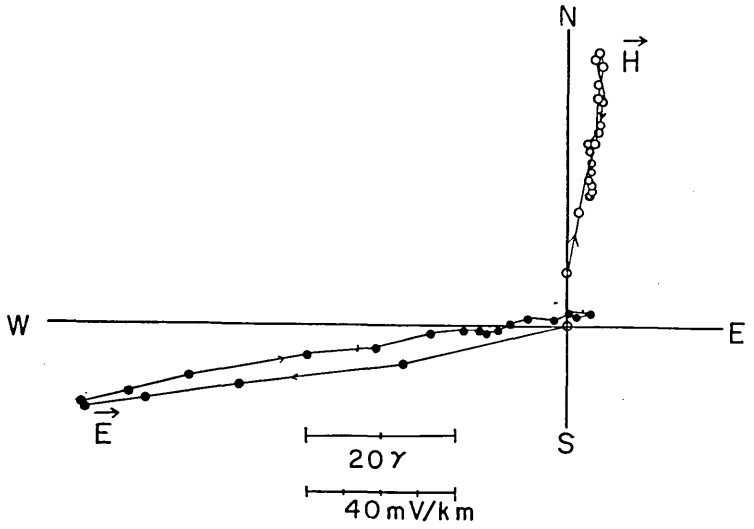

Fig. 13. Hodogram for variation No. 1.

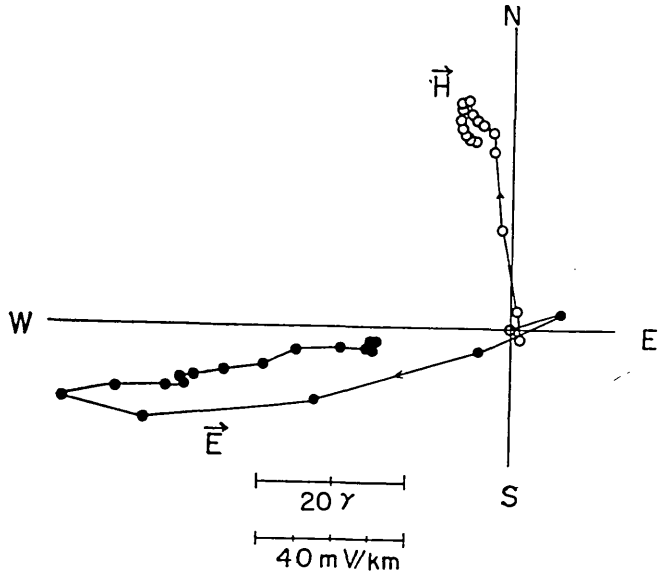

Fig. 14. No. 2.

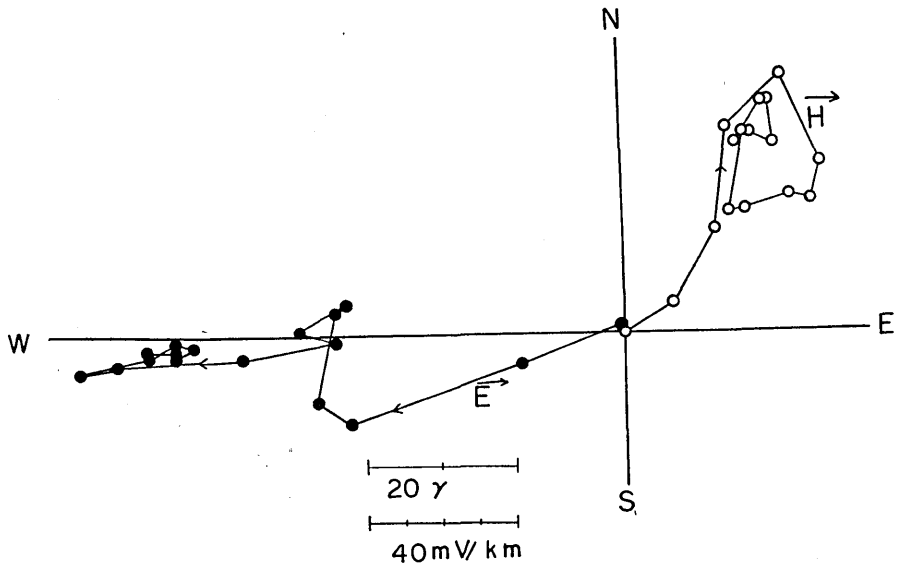

Fig. 15. No. 3.

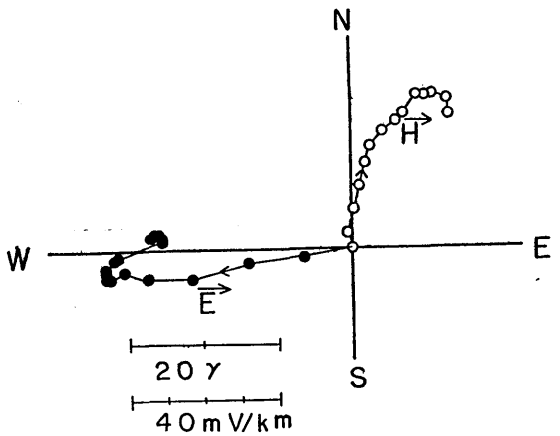

Fig. 16. No. 4.

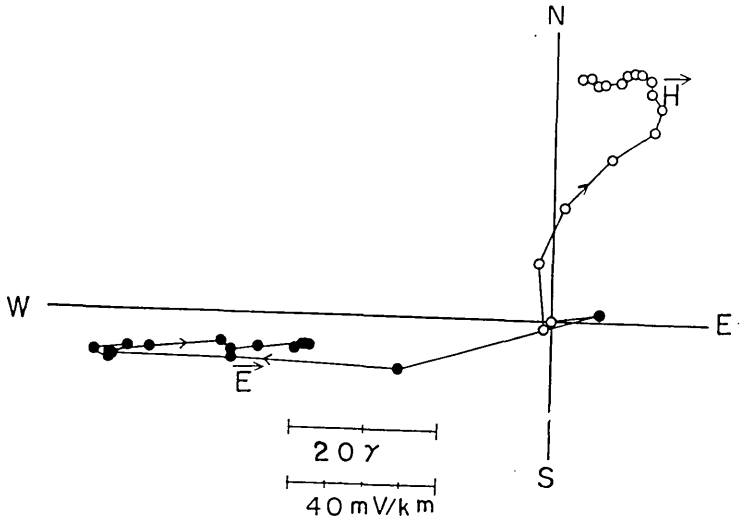

Fig. 17. No. 5.

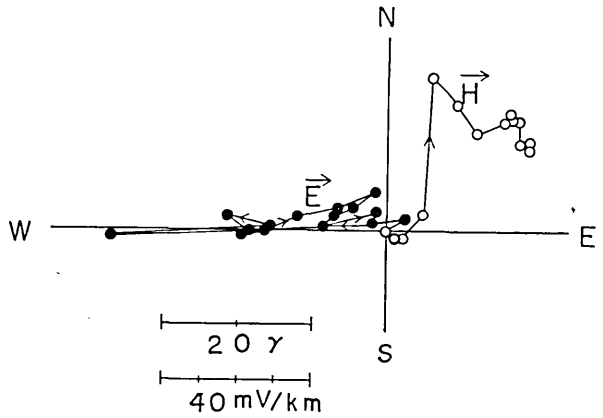

Fig. 18. No. 6.

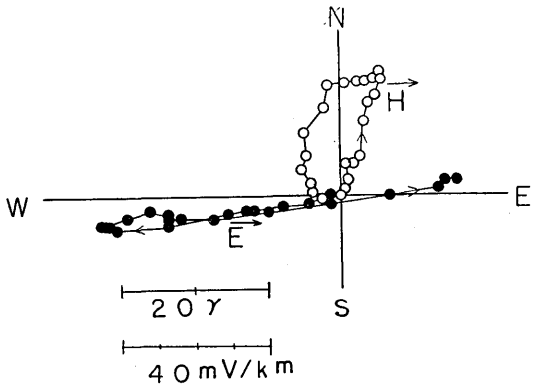

Fig. 19. No. 7.

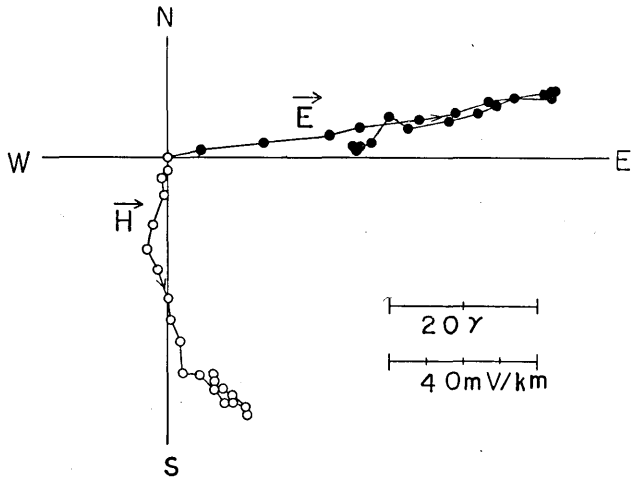

Fig. 20. No. 8.

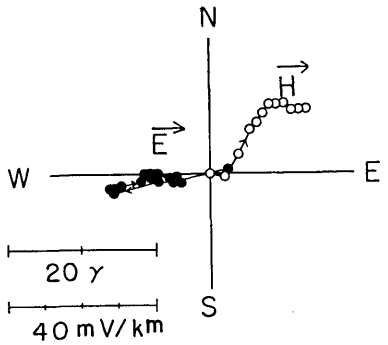

Fig. 21. No. 9.

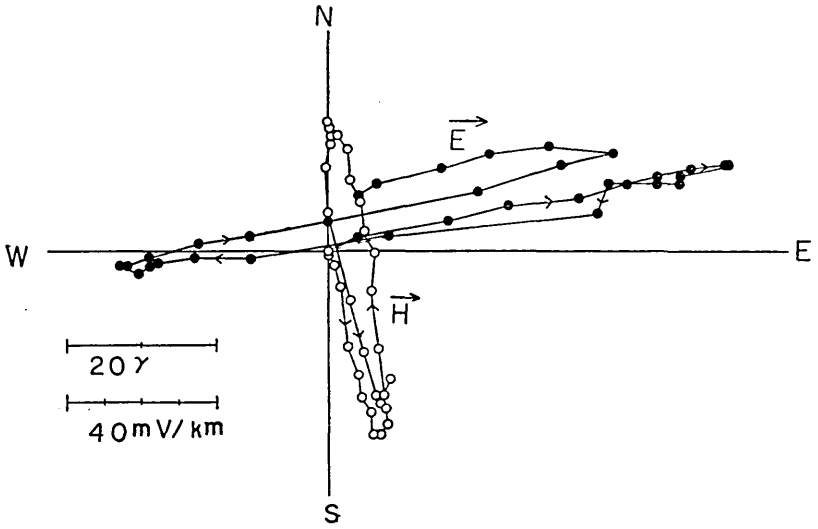

Fig. 22. No. 10.

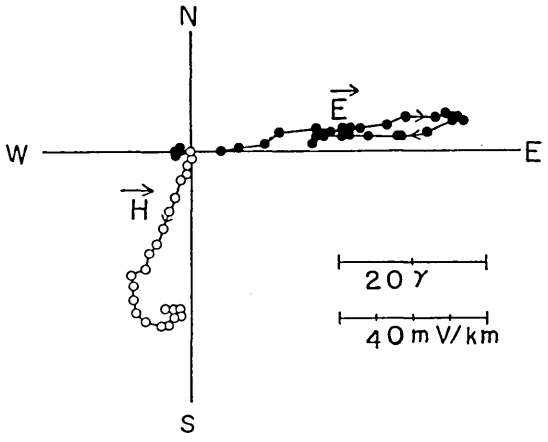

Fig. 23. No. 11.

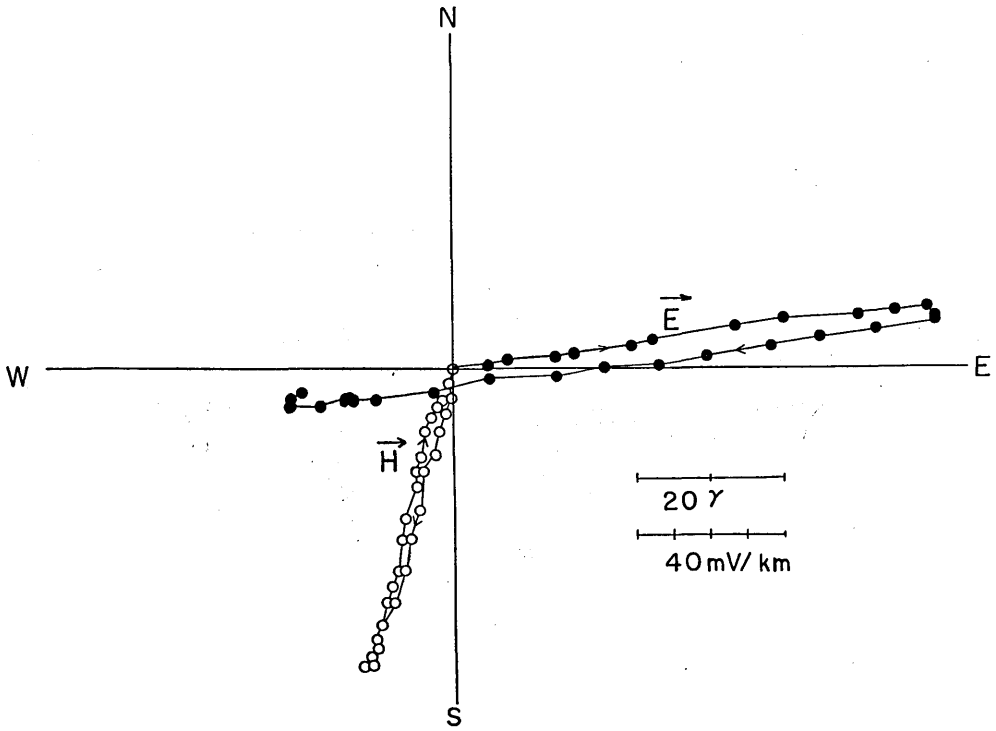

Fig. 24. No. 12.

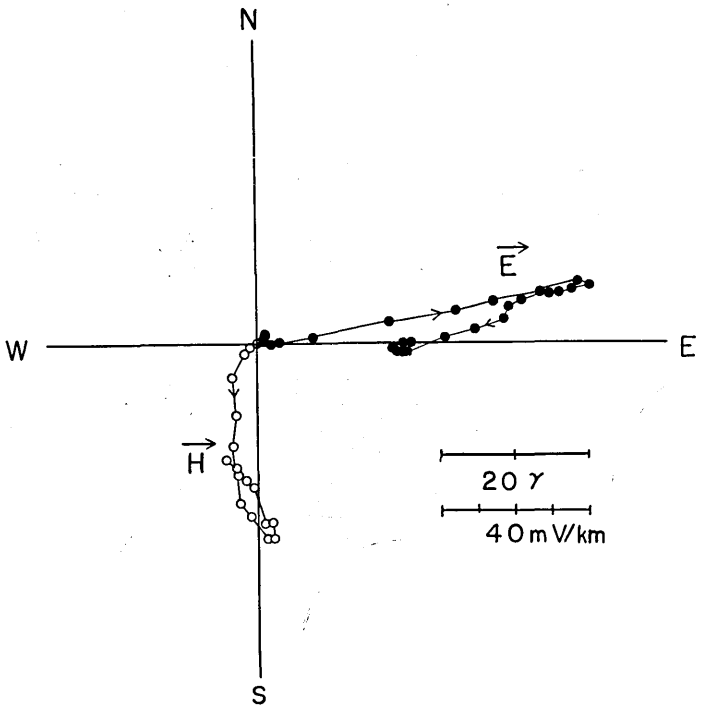

Fig. 25. No. 13.

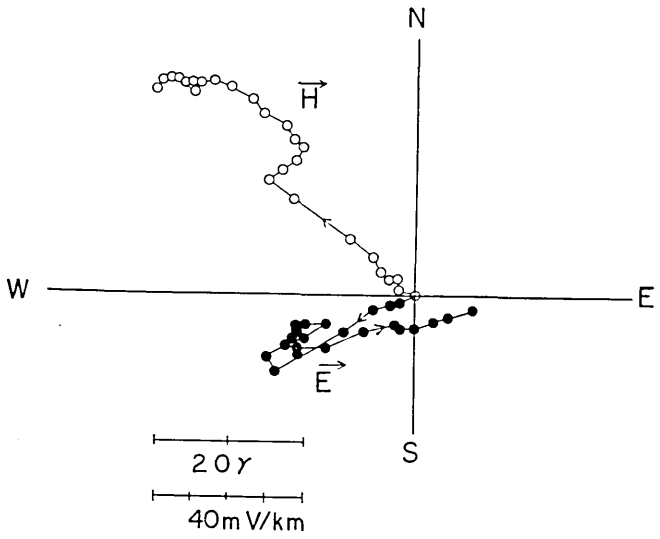

Fig. 26. No. 14.

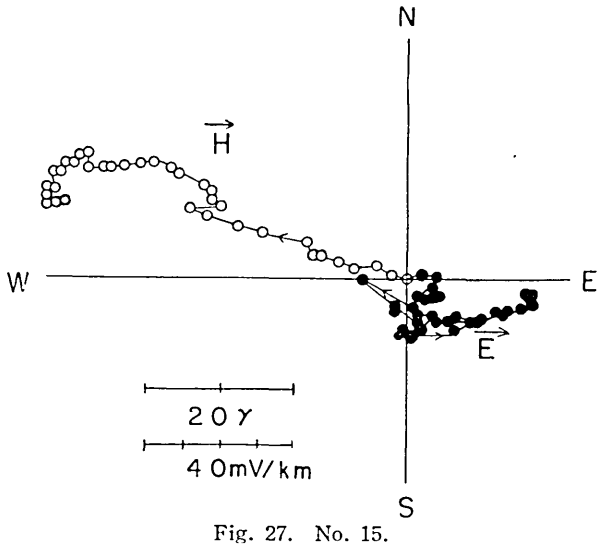

Fig. 27. No. 15.

where

$$\mu=(r/2\pi)(\rho_{yy}\sin^2\theta+\rho_{xx}\cos^2\theta)\ . \tag{39}$$

It is assumed that the influence of the deeper layer is very little for rapid changes as has been shown in Section 5, so that K in the

above is obtained on the basis of (25). Now from (32) and (34), the electric and magnetic fields are obtained as

$$\left.\begin{aligned} E_\xi &= e_0 \frac{\lambda\mu}{\lambda-\mu}(e^{-\mu t}-e^{-\lambda t}) \sin r\eta \\ E_\eta &= -e_0 \frac{\lambda\nu}{\lambda-\mu}(e^{-\mu t}-e^{-\lambda t}) \sin r\eta \end{aligned}\right\} \tag{40}$$

where

$$\nu=(r/2\pi)(\rho_{xx}-\rho_{yy}) \sin\theta \cos\theta \tag{41}$$

and

$$\left.\begin{aligned} H_\xi &= 0 \\ H_\eta &= r e_0\left\{1-e^{-\lambda t}+\frac{\lambda}{\lambda-\mu}(e^{-\mu t}-e^{-\lambda t})\right\} \sin r\eta \end{aligned}\right\} . \tag{42}$$

For small values of t, these expressions reduce to

$$\left.\begin{aligned} E_\xi &= e_0\lambda\mu t \sin r\eta \\ E_\eta &= -e_0\lambda\nu t \sin r\eta \\ H_\eta &= 2re_0\lambda t \sin r\eta \end{aligned}\right\} . \tag{43}$$

As E_ξ, E_η and H_η are given from observational data, μ/r and ν/r can be determined by making use of data at a small numbers of t's of a particular variation. Going back to (39) and (41), $\rho_{yy}\sin^2\theta+\rho_{xx}\cos^2\theta$ and $(\rho_{xx}-\rho_{yy})\sin\theta\cos\theta$ can thus be obtained. If we assume that the variation in the magnetic field is directed to a direction ϕ measured from the north and that the direction of maximum resistivity makes an angle ε with the north-south direction, we obtain

$$\theta=\varepsilon-\phi \tag{44}$$

where ϕ can be determined from the observational results for a particular variation.

It is now possible to determine ρ_{yy}, ρ_{xx} and ε provided we have two sets of μ/r and ν/r or more. Choosing two variations, *e. g.* Nos. 1 and 15, of which directions are widely different from one another, the elements of anisotropy are determined as

$$\left.\begin{aligned} \rho_{xx} &= 1.3\times10^6 \, e.\,m.\,u. \\ \rho_{yy} &= 5.7\times10^6 \, e.\,m.\,u. \\ \varepsilon &= N78^\circ E \end{aligned}\right\} ,$$

so that we see that $\rho_{max.}/\rho_{min.}$ amounts to 4 or thereabouts at Kakioka.

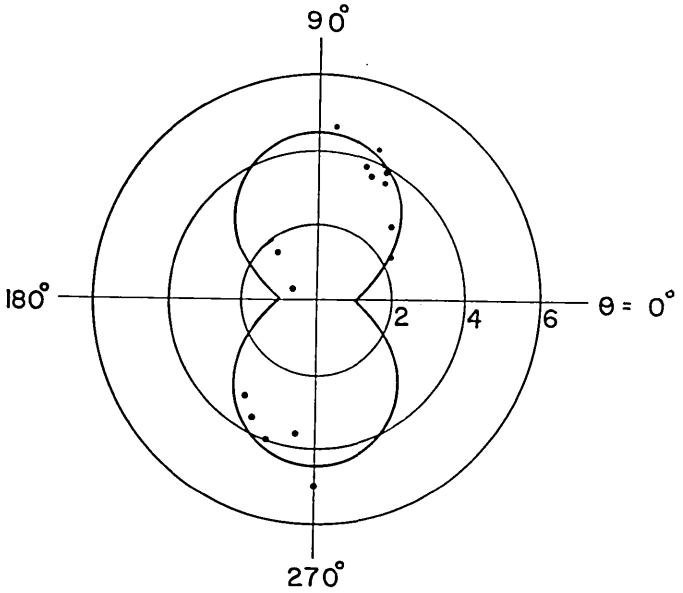

Fig. 28. Directional characteristics of $|E/H|$ in units of $mV/km/\gamma$ for fifteen rapid variations at Kakioka. The curve based on the theory is also shown. $\theta=0°$ denotes the direction of minimum resistivity.

In Fig. 28 is shown $|E/H|$, amplitude ratio of electric and magnetic fields in the horizontal plane, for changes given in Table 1. Meanwhile $|E/H|$, that is expected from the theory by making use of the ρ_{xx} and ρ_{yy} determined in the above, is also shown as a function of θ. Although the scattering of observed values is fairly large, the general feature of the directional characteristics of the electric field may be said to be accounted for by the present theory. It might be worthwhile to point out that $|E/H|$ does not depend on r or on the wave-length of variation so long as t is assumed to be small as can be seen in (43).

7. Concluding remarks

A theory of electromagnetic induction in an anisotropic plane sheet is developed in this paper. It is made clear by the theory that the direction of the maximum electric field in the sheet does not generally

agree with those of induced electric current or the maximum resistivity.

The intensity of induced current depends on the direction of inducing magnetic field though it takes almost the same value for any direction in the case of a rapid change. The direction of induced current is always perpendicular to that of inducing magnetic field. The effect of highly conducting layer in the deep becomes appreciable for slow changes only when the wave-length of the fields is much greater than the depth of the layer.

The application of the present theory to rapid changes observed at Kakioka Magnetic Observatory proves that the relationship between magnetic and electric fields may be approximately accounted for as far as the beginnings of the changes concerned.

It may be said that we can describe earth-currents at a certain observatory as electromagnetic induction within an earth approximated by an anisotropic plane sheet over a non-conductor which is underlain by a uniform semi-infinite conductor. However, the reason why there is such an anisotropy is another problem though it has been presumed to be caused by some kind of topographical or geological control of electric field induced. A theory[11] concerning the relation between non-uniformity and anisotropy in the earth's conductivity will be advanced later.

---

36. 地表付近の電気伝導度が異方性を有する場合の電磁感応

地震研究所 力武常次
東京大学大学院 地球物理学専門課程 沢田宗久

地電流のふるまいと関連して Fig. 1 のような表面に電気伝導度の異方性をもつモデルを考えた．表面層の厚さを 10 *km*，電気伝導度が直角方向に 10 倍ほど違うこと，insulator の厚さを 400 *km*，field の波長を 1000 *km* と仮定し，周期が 1 分から 24 時間までの変化に関し，uniform conductor の電気伝導度が 0 の場合および 10^{-12} *e. m. u.* の場合について電磁感応の計算を行なつた．それによると，磁場と直角に誘起される電場は，周期の短いものについては著しい異方性を示すが，周期の長いものについてはさほどの異方性を示さないことがわかつた．誘起される電場の方向は，一般に誘起される電流の方向（外部磁場につねに直角）とも抵抗の最も大きい方向とも異なることが結論される．

この理論を柿岡における観測結果に適用して，電気伝導度の最大値と最小値の比が 4 程度であることを見出した．

---

11) T. YUKUTAKE and T. RIKITAKE. To be published in *Bull. Earthq. Res. Inst*